NETWORK BIOLOGY APPROACHES TOWARDS THE IDENTIFICATION OF PREDICTIVE CANCER BIOMARKERS

Thesis booklet

Klára Schulc, M.D.

Molecular Medicine Doctoral School

Semmelweis University

Supervisors:	Péter Csermely, Ph.D., D.Sc. Dániel Veres, M.D., Ph.D.
Official reviewers:	X.Y, M.D., Ph.D. X.Y, M.D., Ph.D.
Head of the Complex Examination Committee:	Csaba Bödör, Ph.D., Habil.
Members of the Complex Examination Committee:	Gábor Turu, Ph.D. Máté Szalay-Bekő, Ph.D.

Budapest
2026

1. Introduction

"Down to their innate molecular core, cancer cells are hyperactive, survival-endowed, scrappy, fecund, inventive copies of ourselves."

— Siddhartha Mukherjee, The Emperor of All Maladies: A Biography of Cancer

1.1. The development of cancer

Cancer is a disease, where genetic changes lead to sustained proliferation. Hallmarks of cancer include angiogenesis, immune evasion, invasion and metastasis. Environmental factors lead to somatic evolution and adaptation, affecting the cell's whole regulatory machinery. System-level tools help understanding these changes. One example is the MAPK pathway, as its dysregulation leads to excessive proliferation. Cancer drugs target this pathway, but there are no good biomarkers for longitudinal monitoring. Carcinogenesis is well researched in colon cancer, where changes occur through decades. The normal–adenoma–carcinoma sequence accumulates mutations, starting with APC, followed by KRAS and finally, TP53 and SMAD4. These lead to global network changes, which system biology can better understand. Adding colon adenoma to a 3-step carcinogenesis model, which was not done before, can highlight differences.

1.2. Therapy resistance

Therapy resistance is causing ineffective treatments. toxicity, and excessive costs. It can be intrinsic or acquired. Intrinsic resistance may be caused by pre-existing mutations, signalling patterns or pharmacokinetics, while for acquired resistance, it can be new mutations, drug efflux pumps, microenvironmental changes or pathway cross-talks. Resistance can be described as the forgetting of networks, as the cell 'forgets' pathways and learns new ways of signalling, where IDPs participate with their flexible conformation. This complexity sets the stage for system-level analyses. The question is how we can detect the cellular forgetting with sensitive markers and how to tackle the adaptation by rather causing the forgetting of the unwanted signalling processes.

1.3. Biomarkers in cancer therapy

Predictive biomarkers must be trusted for clinical decision-making; thus, they should be sensitive, specific, and easily detectable. They can be DNA, RNA, proteins or metabolites. Detection can be from the tumour or with liquid biopsy. Biomarker discovery can be by high throughput sequencing, bioinformatic screening, or laboratory experiments. IDPs are essential in cancer signalling due to their flexible structure, thus, targeting them is challenging. We hypothesise that IDPs can be good biomarkers, and they should be screened. LncRNAs were previously considered 'junk' RNAs, but they are attractive biomarkers because many are stably present in body fluids, a key for non-invasive liquid biopsies. Despite their function is not clear, we hypothesise biomarker identification is still possible, and they may be suitable for longitudinal decision support. Identifying them is a multi-step process concluding in clinical validation.

1.4. *In silico* methods to understand cancer signalling

Network motifs are important in perturbation propagation, and their co-regulation is stronger than a simple connection. Network centralities show the influential nodes in the network. Bridgeness centrality shows the signal transductors between modules. IDPs also interact with central nodes, creating an interface for the rest of the network. This calls for the screening of network motifs for biomarkers, with the help of IDP annotations. Machine learning can contribute by predicting based on previous knowledge. Tree-based methods and feature importances provide interpretability, while applying cross-validation can test for overfitting. Harmonising multiple models create more robust predictions, which should be followed with prediction validation. We hypothesised that the combination of rich topology data and biological attributes can lead medically relevant biomarker predictions. This provides potential biomarkers ready for further testing and brings us closer to understand predictive biomarkers on a network science level.

2. Objectives

2.1. Overall objective

The main objective was to understand signalling changes in cancer better with the tools of network science, machine learning and experimental biology, while identifying predictive biomarkers for cancer targeted therapeutics.

2.2. Specific objectives

As this PhD research included collaborative work and an international research scholarship, multiple different projects tackling cancer signalling and biomarker detection were conducted with different methodologies. We highlight the value of these methodologies by using examples from the MAPK pathway throughout this thesis, which is a core signalling pathway governing proliferation in cancer cells.

1.) Network topology changes in cancer development

For the colon carcinogenesis modelling project, the goal was to assess system-level changes during transition from healthy colon through colon adenoma to colon carcinoma from a network topology standpoint.

2.) Network-based tool to predict cancer biomarkers

The goal of the MarkerPredict project was to create a network-based biomarker prediction tool using network topology data and biological attributes, including IDP annotations for targeted cancer therapies. The goal was also to assess the following hypotheses: a) network motif members are more likely to be biomarkers of their neighbours b) IDP proteins are more likely to be biomarkers.

3.) LncRNA biomarker signature for MAPK inhibitor cancer therapies

The goal of the liquid biopsy lncRNA project was to find a pan-cancer lncRNA biomarker signature for MAPK pathway activity to detect MAPK inhibitor therapy effectiveness.

3. Methods

In this section, we describe methods used during the various projects mentioned in this thesis. Many of these were published by the candidate and her collaborators.

3.1. Network construction and topology analysis

A network's definition relies in its nodes and edges. For protein-protein interaction networks, it is the interactions, while for signalling networks, only regulatory connections. For the motif analysis, CSN, SIGNOR and ReactomeFI networks, the directed edges were selected. For the colon development study, the CSN network was weighted using healthy, adenoma and carcinoma data (n=128, 131 and 178), collected with Borbála Kovács. RNA normalization and median aggregation was conducted by Sebestyén Kamp and János Molnár. Edge weights were calculated by:

(1)

$$Link\ weight_{AB} = \log_{10}\ (Abundance_A x\ Abundance_B)$$

There is higher chance of interaction with higher abundance, and logarithmization reduces outliers. Multiple network parameters, such as **bridgeness** and **betweenness** centrality were used, mostly calculated with *NetworkX* and *ModuLand*. **Network diameter** is the longest shortest path in the network, here calculated with *a)* directed network *b)* undirected *c)* replacing neutral edges with bidirectional ones, with negative logarithmic, reciprocal transformation or inversion on the edge weights. Dijkstra's algorithm was used, first developed by Zsolt Nagy, then adapted by the candidate.

Three-nodal motifs were identified with the FANMOD program. **Triangles** were further analysed, with **unbalanced triangles** and **cycles**. Modules were identified with the *ModuLand* plugin, partially ran by Borbála Kovács. It calculates the assignment of nodes based on influence functions, allowing module overlaps. Nodes having the largest community centrality organise the module.

3.2. Protein annotation in triangles

Proteins in the identified triangles were annotated for further analysis. Disordered regions were determined by three different methods, *DisProt*, the gold-standard, and *AlphaFold*

and *IUPred*, two IDP prediction methods. Onco-therapeutic targets were found in the *My Cancer Genome* database, and the Target Central Resource Database was used to identify preclinical targets. All the 4550 **neighbour-target pair** was identified in the triangles to construct the train and test datasets. The *CIViCmine* database defined **predictive biomarker** as a protein helping to predict response to a certain drug. When the neighbour of a target served as a predictive biomarker for the drug, we used them as **positive controls**. We defined a **negative control** set from neighbour proteins not in *CIViCmine*, with randomly selected pairs for the DisProt-only dataset. These formed the training dataset, while the remaining pairs were used for prediction.

3.3. Machine learning

Random Forest (RF) and XGBoost (XGB) were used, with optimised hyperparameters. The training dataset includes topological parameters, such as motif annotations, edge types and centrality values, and biological parameters such as IDP annotations and drug target annotations. Performance was evaluated with cross-validation methods, with various metrics calculated. Final predictions were made on unclassified pairs, for all database- and network-specific models. Feature importances were identified with the *SHAP* package. The **MarkerPredict** GitHub package, established with Gábor Kovács, contains the codes and input data and is applicable to other networks and biological problems (https://github.com/klari98/MarkerPredict).

3.4. Biomarker Probability Score (BPS) calculation

Biomarker Probability Score (BPS) estimates neighbour's biomarker potential for the target's inhibitor. It was calculated from the probabilities of the final prediction from 32 separate models. BPS was calculated according to this formula:

(2)

$$BPS(p) = 1 - \frac{\left(\frac{\sum_{i=1}^{n} R_{p,i}}{n}\right)}{m-1}$$

where *R* is the rank of the probability of class 1 for the pair in the given prediction *i*, *n* is the total number of predictions and *m* is the total number of pairs. This was calculated 4 times for different IDP annotations. BPS correlates well with the label (see Figure 1.).

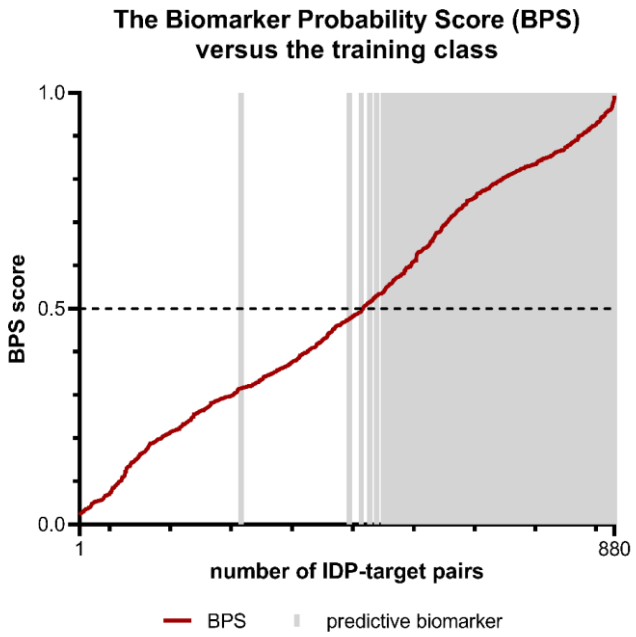

Figure 1. The BPS score versus the original training label. *BPS score correlates well with original labels, showing that the score is suitable to use on new predictions. This figure is in the candidate's publication as Figure 1E and included with the permission of co-authors.*

3.5. Methods in pathway specific lncRNA identification

Lung (A549, HT1299) and liver (HuH7, Hep3B) maintained by Patrizia Birner) cell lines were provided by Prof. Kai Breuhahn. Cell lines were in DMEM 10% FCS 1% penicillin/streptomycin medium and were kept at 37 °C with 5% CO2. Viability detection was performed after 1h with 10% rezonium. Drug treatments were performed with trametinib and binimetinib (MEK inhibitors) and ulixertinib and MK-8353 (ERK inhibitors) alongside with the AKT inhibitor AKTVIII, with DMSO control. Cells were treated with gene-specific siRNAs according to the Opti-MEM protocol, with non-silencing siRNA control. Protein isolation, Western blotting, RNA extraction and RT-qPCR was conducted as described by Prof. Kai Breuhahn. Multiple lncRNA primers were tested for each target, designed on exon-exon junctions. LncRNA candidates with working primers were used for further analysis. RNA sequencing including lncRNAs was performed on one NSCLC (A549) and one HCC (Hep3B) cell line after 3 hours of

trametinib or MK-8353 treatment or DMSO control by the BGI company (Hong Kong). RNAseq preprocessing was conducted by Carsten Sticht. lncRNA candidates were identified among the downregulated lncRNAs. The prognostic value of lncRNA candidates was evaluated on TCGA HCC and NSCLC data.

4. Results

4.1. Key network topology changes in the development of colon adenocarcinoma

Network science was used to model colon cancer development with the CSN network and RNA microarray of healthy colon, adenoma and carcinoma. Changes in global and local network attributes highlighted important changes. The research was already published, in collaboration with Borbála Kovács, Zsolt Nagy, Sebestyén Kamp and János Molnár.

4.1.1. Network diameter

On the network models, multiple network diameter calculations were conducted, handling the networks as a) undirected, b) directed and c) the mixture of the two. As the calculated edge strengths represent connection strengths and the used Dijkstra algorithm handles them as distance, values were reversed by a) negative logarithmic transformation, b) reciprocal transformation, c) inversion, as first developed by Zsolt Nagy and adapted by the candidate. Adenoma showed the largest, and carcinoma the smallest diameter. The findings were reproducible and robust under noise. The increased diameter in adenoma suggests a less compact network architecture, while the reduced diameter in carcinoma may reflect an adaptive strategy to enhance information flow.

4.1.2. Therapy-related pathways

EGFR-, VEGFR-inhibitors and immune checkpoint inhibitors are used in colon cancer, thus, these pathways were analysed, defined by Gene Ontology terms. The mismatch repair pathway was not well represented in the CSN network, which is enriched for signalling-related proteins. Median abundance of VEGFR pathway proteins were the highest in the carcinoma dataset, while the median weighted degree was the highest in the normal network for EGFR and VEGFR (see Figure 2.). This may be due to the higher-expressed neighbours of the pathway proteins, and EGFR is important in the healthy alimentary tract too. Most nodes clustered into the RAC1 module, the largest module in the network, as identified by Borbála Kovács. These pathways do not form distinct modules because they are highly intertwined with the rest of the graph.

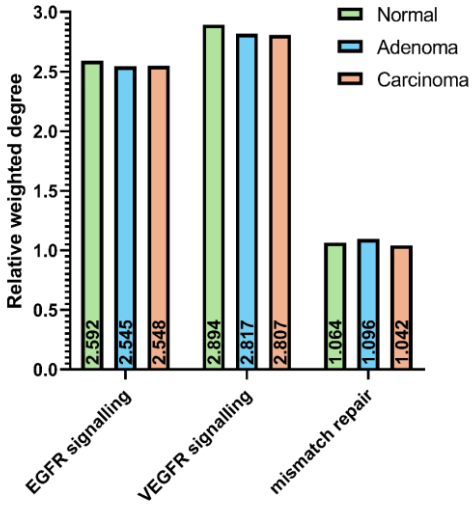

Figure 2. Median relative weighted degrees of therapy pathway related nodes. *Weighted degrees were calculated as the sum of the edge weights. Relative weighted degrees were the quotients of the weighted degrees of the pathways and the whole network. The data was published as Table S10 in the candidate's publication, shown with the co-authors' approval.*

4.1.3. The MAPK pathway during colon carcinogenesis

As about half of colon cancer patients have MAPK mutations, it was analysed in the network models (see Figure 3). However, we note that the effect of MAPK pathway changes might be on posttranslational and downstream levels, which is difficult to assess with this model. The *'MAPK cascade'* Gene Ontology term were analysed, and ~80% of them belongs to the RAC1 module. Their relative weighted degree is decreasing throughout carcinogenesis. However, several key MAPK components' weighted degree increased from normal through adenoma to carcinoma.

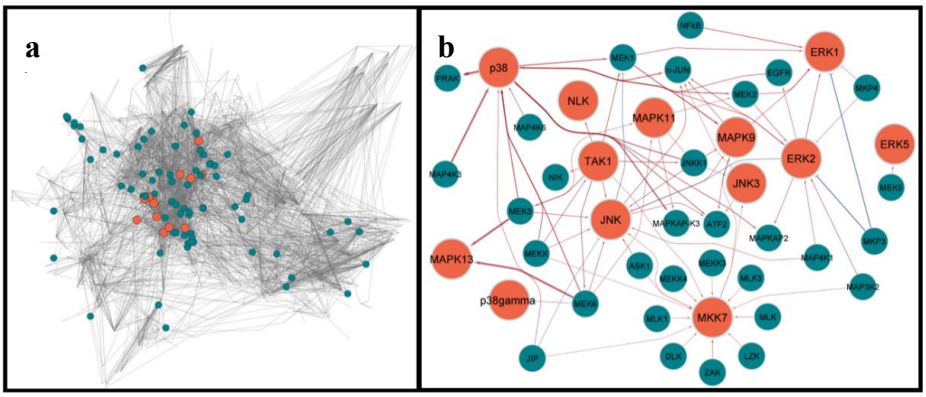

Figure 3. The MAPK pathway in the colon carcinoma network. *Blue nodes belong to the 'MAPK cascade' and orange nodes to the narrower 'MAP kinase activity' GO terms.* ***a)*** *EntOpt visualisation of the network with the highlighted pathway.* ***b)*** *The MAPK cascade subnetwork.*

4.2. MarkerPredict: Predicting biomarkers to cancer drugs

Motif analysis and graph-based models lead to the **Biomarker Probability Score (BPS)**, a powerful tool in biomarker identification (see Figure 4.). It was published with Dániel Veres, Péter Csermely, and Gábor Kovács, see https://github.com/klari98/MarkerPredict.

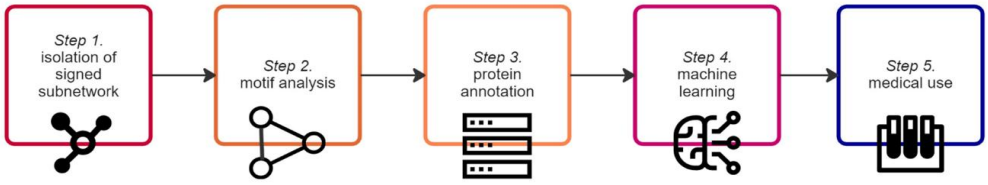

Figure 4. The MarkerPredict process. *After network construction and motif-analysis, annotation was conducted for the input dataset. The final predictions were sorted by medical relevance. This was published as Figure 1A, shown with the co-authors' approval.*

4.2.1. The enrichment of IDPs in triangles of therapeutic targets

Triangles containing DisProt-defined IDPs and drug targets were analysed as signalling "hot spots." Unbalanced triangles were overrepresented, whereas cycles were only overrepresented in the CSN and SIGNOR networks. Importantly, IDP–target triangles appeared far more frequently than expected by random chance. This enrichment held true not only for DisProt-defined IDPs but also for AlphaFold-based and IUPred-predicted IDPs (a range of 3-11.91x enrichment in total). We hypothesised that IDPs in the same triangle as a drug target (**"IDP–target pairs"**) may be predictive biomarkers. To expand the analysis, we also included all neighbours of drug targets (**"neighbour–target pairs"**).

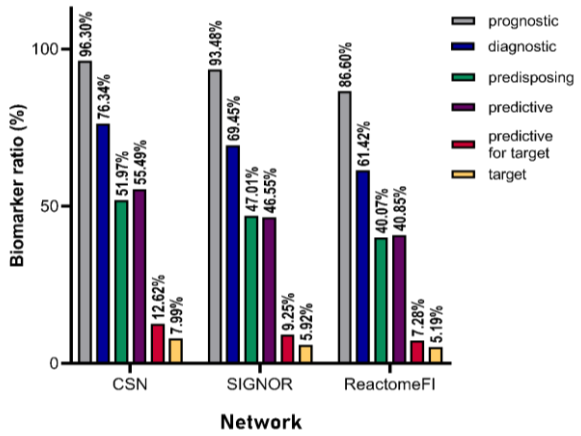

Figure 5. Biomarkers and targets of neighbours in target-neighbour triangles. *Most of the neighbours (86.6% - 96.3%) are CIViCmine biomarkers, many is a predictive biomarker of a drug targeting their neighbour. This was published as Figure 1C, shown with the co-authors' approval.*

In the 4,550 pairs, more than 86% of IDPs were some type of biomarkers in the CIViCmine database (see Figure 5.). Predictive biomarkers for a drug targeting its triangle partner were manually reviewed and designated as positive controls, and negative control was neighbours not in CIViCmine and random pairs.

4.2.2. MarkerPredict is a powerful tool for biomarker prediction

Random Forest and XGBoost was trained on 880 pairs, the rest was for prediction. Performance was evaluated with splits and cross-validation (see Figure 6.). All models achieved strong metrics; even on the smaller DisProt data. Random Forest models performed worse, such as models of the smallest CSN network. Accuracy was between 0.7-0.96. We defined the Biomarker Probability Score.

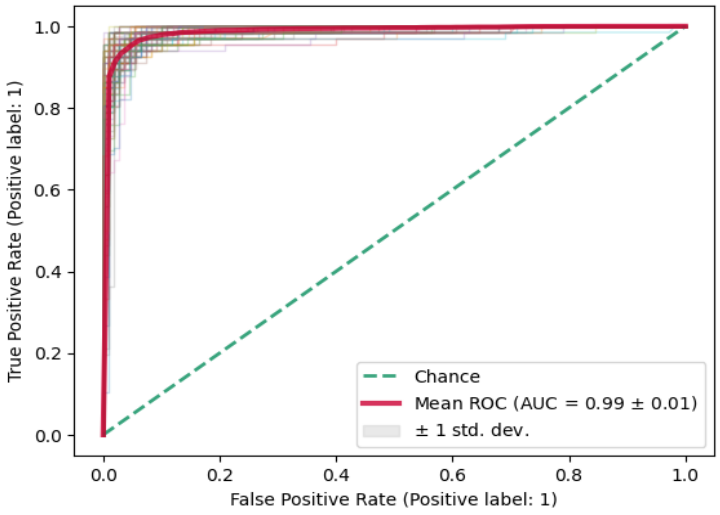

Figure 6. The ROC curve of 100 5-fold cross-validation of the XGBoost model. *The model had excellent performance, with an AUC of 0.99±0.01 (shown with red). Other models also showed high performance. This was published as Figure 1D, shown with the co-authors' approval.*

SHAP values indicate that IDP databases are influential inputs, with centrality measures and motif analysis. Pairs with low or moderate disorder content were more likely to be predicted as biomarkers, whereas for IUPred short predictions, developed for short regions, it was reverse. The exact translation of this varies on the disorder prediction tool.

4.2.3. Predicted biomarkers with biomedical relevance

We calculated the BPS Score for each pair across all IDP annotations (see Sections 3.4–5). BPS effectively unified probability estimates. Using a threshold of BPS > 0.5, 2084 pairs were potential predictive biomarkers, and 426 pairs in all four IDP-specific analyses.

For many high-BPS pairs, evidence supported the predictions (see Table 1.). The top predictions exhibit low to moderate – but not zero disorder content.

Table 1. Top 5 predictive biomarker predictions. *BPS was calculated from 8 models. Therapies are from My Cancer Genome. Supporting literature is from PubMed. Preclinical and clinical articles were collected. This table's data was published as part of Table 1, shown with the co-authors' approval. This table only shows the top 5 predictions of all IDP annotations model.*

No	Bio-marker Proba-bility Score (BPS)	Neigh-bour name	Annotation disorder content (%)				Target name	Inhibitor(s) of target	Supporting literature
			DisProt	*AlphaFold*	*IUPred (long)*	*IUPred (short)*			
ALL ANNOTATIONS									
1.	*0.998*	**LCK**	*7.1%*	*11%*	*3.1%*	*3.9%*	**EGFR**	afatinib, cetuximab, erlotinib, gefitinib, lapatinib, necitumumab, osimertinib, panitumumab, vandetanib	*Clinical:* Pizzamiglio et al., 2021
2.	*0.991*	**LCK**	*7.1%*	*11%*	*3.1%*	*3.9%*	**PDGFRB**	regorafenib, axitinib	
3.	*0.990*	**ITGB1**	*5.9%*	*3.8%*	*5%*	*6.6%*	**EGFR**	afatinib, cetuximab, erlotinib, gefitinib, lapatinib, necitumumab, osimertinib, panitumumab, vandetanib	*Preclinical:* Gu et al., 2025
4.	*0.990*	**ERK1**	*6.1%*	*6.5%*	*6.6%*	*12%*	**FGFR3**	ponatinib	*Preclinical:* Matsuda et al., 2016
5.	*0.987*	**STAT1**	*5.5%*	*6.1%*	*6.8%*	*6.9%*	**EGFR**	afatinib, cetuximab, erlotinib, gefitinib, lapatinib, necitumumab, osimertinib, panitumumab, vandetanib	*Preclinical:* Yang et al., 2025 *Clinical:* Srivastava et al., 2016

Predictive biomarkers of BRAF and MEK1/2 inhibitors are BRAF and NRAS/KRAS mutations, but they only detect intrinsic resistance. To identify more markers, the 139 neighbour-MEK1/2 pairs were added, and the MarkerPredict script were re-ran. The new scores are only used here (see Figure 7.). Several potential predictive biomarkers were identified. ERK1 had a high BPS score for both BRAF, MEK1 and MEK2, corresponding with it is a frequent MAPK pathway readout. Several other MAPK pathway members were also predicted, such as RAF1, ERK2, SHC1, SOS1, SRC and RAC1. Many predicted biomarkers have supportive evidence. ERBB2 has been shown to drive resistance to BRAF inhibitors in BRAF mutant tumours. GSK3B activity is associated with reduced vemurafenib response. PRKCA and PIK3R1 are markers of MEK inhibitors in cell lines.

YWHAZ (14-3-3ζ) is the only 14-3-3 protein predicted as biomarker for BRAF and MEK1/2 inhibitors. 14-3-3 proteins bind and regulate BRAF/MEK complexes in both the autoinhibited and the active status. YWHAZ overexpression associates with worse survival in various cancers. It promotes upstream MAPK associated signalling, and its genetic blockage disrupts ERBB2 and PI3K signalling. There are efforts to inhibit YWHAZ, however, there are no drugs in clinical phase yet. It has 4.9% disorder content, and it is difficult to design drugs for IDPs. The role of YWHAZ in cancers and MAPK pathway highlights its biomarker potential, which needs further validation.

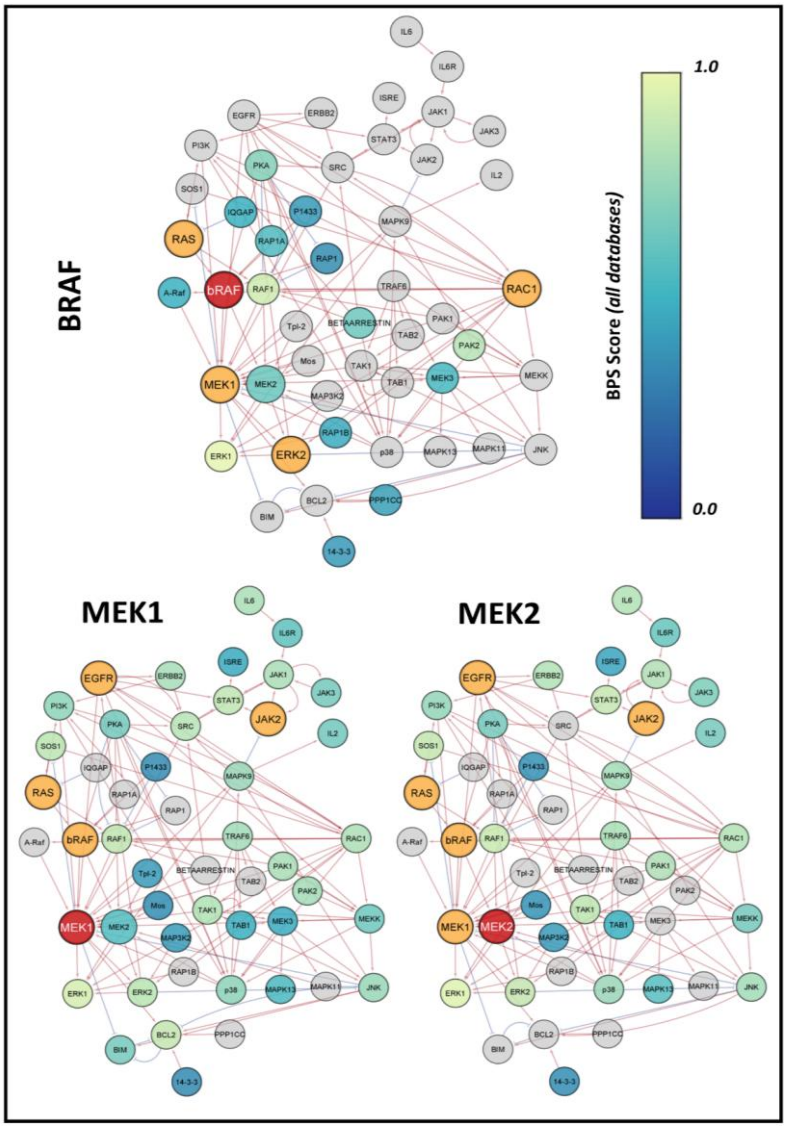

Figure 7. The BPS scores for MAPK pathway inhibitors. *The CSN network was visualised, the subnetwork of MEK1/2 and BRAF motifs were created. Positive edges are shown with red; negatives are with blue. Targets are shown with red, defined predictive biomarkers with orange. 3 separate visualisations show the BPS for BRAF, MEK1 and MEK2. Non-pairs showed with grey.*

4.3. A pan-cancer MAPK pathway lncRNA signature

First, we searched for the optimal cell lines, drugs and timepoints of optimal MAPK pathway downregulation. LncRNAseq was performed in an in an external laboratory, followed by the identification of lncRNA candidates and confirmation experiments. This project was supervised by Prof. Kai Breuhahn, and experiments were conducted with Patrizia Birner. The theoretical pipeline was developed by Fabian Rose.

4.3.1. Optimal conditions for effective MAPK inhibition

For a pan-cancer lncRNA signature, cell lines of two different cancer types were. To ensure that the results are specific to the MAPK pathway, drugs on two separate point of interference were tested. Viability testing was used to find effective but not lethal inhibition. Western blotting was performed (see Figure 8.).

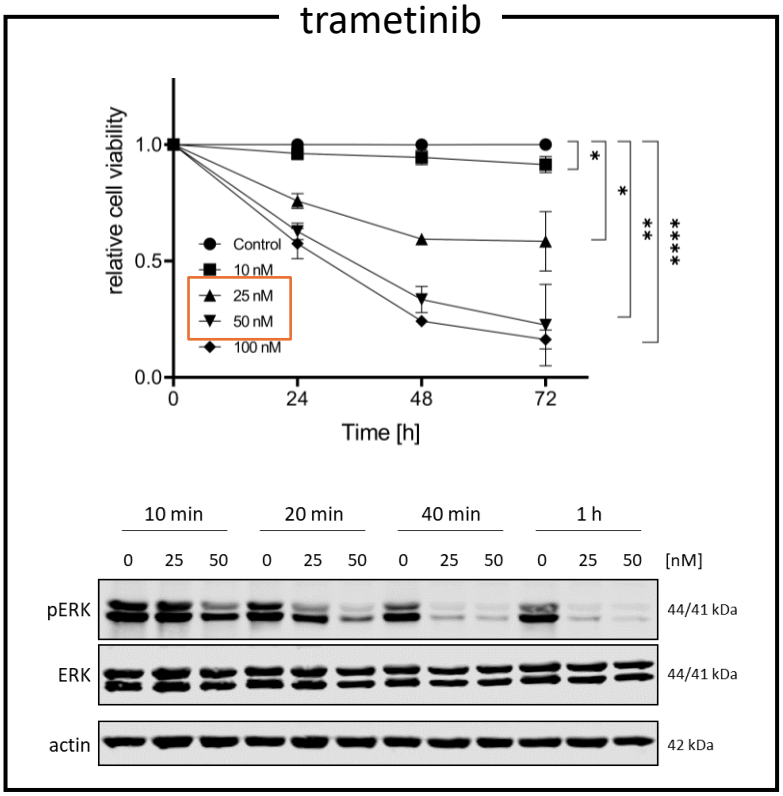

Figure 8. The effect of trametinib inhibition on Hep3B HCC cell line. *Viability testing was performed with DMSO control, the ones with medium viability were selected. Effective inhibition was confirmed with Western blotting. Actin was used as control. The same experiments were performed with MK-8353, binimetinib and ulixertinib and with the cell line A549. Mann-Whitney-tests were performed to assess significance. Conditions achieving the strongest MAPK pathway inhibition were later used to create MAPK pathway inhibited samples for lncRNA sequencing.*

RT-qPCR was performed to detect the MAPK target mRNAs DUSP6 and SPRY2, downregulating from 3 hours of treatment. The conditions of the most effective inhibition were *a)* cell lines A549 and Hep3B, *b)* trametinib 25nM, MK-8353 300 nM, *c)* treatment time of 3 hours. Samples were prepared and sent to lncRNA sequencing.

4.3.2. LncRNAseq data analysis and experimental confirmation

RNAseq analysis and lncRNA candidate selection was performed. Downregulation of MAPK genes and lower MAPK Pathway Activity Score supported that the inhibition worked. 35 overlapping downregulated lncRNAs were identified. Primers were designed for the candidates, and confirmatory RT-qPCRs were performed (see Figure 9., names hidden due to the possibility of a patent). These results were confirmed on four different cell lines and treatments, siRNA inhibition of ERK, and starvation experiments.

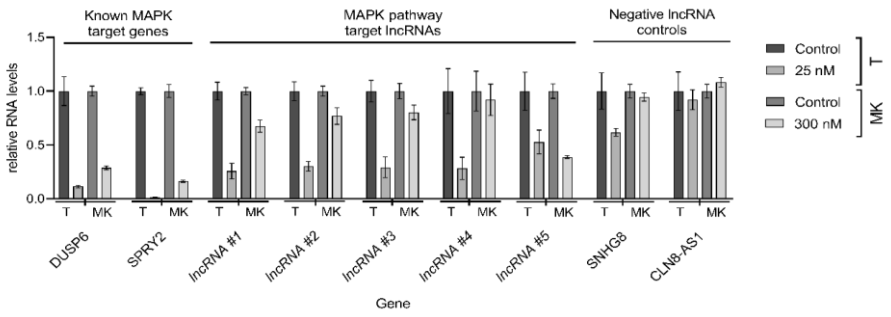

Figure 9. Confirmation RT-qPCR of the lncRNA biomarker panel. *Names are hidden due to the possibility of a patent. This confirms the downregulation of the lncRNA candidates due to MAPK pathway inhibition. This was repeated for sixteen replicates altogether.*

The pathway specificity of the panel was confirmed with AKT and YAP inhibition. 16 known MAPK transcription factors were tested to find regulators of our lncRNAs, and NFAT4 and STAT3 shown to regulate *lncRNA #1*. Altogether, a MAPK-pathway specific lncRNA-panel was identified, with potential clinical potential.

4.3.3. Survival analysis on TCGA data

The prognostic value of our panel was evaluated HCC and NSCLC data by the TCGA Research Network. Tumours have significantly higher expression than healthy tissues, however, expression did not predict survival. As there is no treatment information, we cannot evaluate the predictive biomarker value. Higher tumor expression may help detectability. This panel needs further preclinical and clinical validation.

5. Conclusions

To summarise, here we showed that experimental and *in silico* methods are both helpful to identify key signalling changes and cancer biomarkers. However, while experimental research typically requires a previously well-established question, the high-throughput characteristic of network science and machine learning allowed us to perform mass identification of promising predictive cancer biomarker candidates.

1.) Key signalling changes such as the less-organised then re-organised information flow were identified with the modelling of colon cancer development, represented by growing then decreasing network diameter and average shortest path length in the normal-adenoma-carcinoma sequence.

2.) MarkerPredict, a pan-cancer machine learning biomarker prediction tool was created using network topology data and protein annotation, and tested with various cross-validation methods, showing high performance. A Biomarker Probability Score ranking predictions of 32 different models identified 2084 potential cancer biomarkers.

3.) MarkerPredict showed that more co-regulatory motifs a protein pair participates in, the more likely one can be a predictive biomarker for the other's inhibitor. High centrality values are also attributes of cancer biomarkers. IDPs with low to moderate disorder content can be effective biomarkers.

4.) The identified 2084 predictive biomarker candidates show promise in clinical use, thus require further research and clinical validation to finally help therapeutic decision-making and personalised oncology. Their potential was shown through the example of the 14-3-3ζ protein, a potential biomarker of MAPK pathway inhibitors.

6. Bibliography of the candidate's publications

1. **Schulc K**, Nagy ZT, Kamp S, Molnar J, Veres DV, Csermely P, et al. Modular Reorganization of Signaling Networks during the Development of Colon Adenoma and Carcinoma. J Phys Chem B. 2021;125(7):1716-26. , IF= 2.9, Q1
2. Veres DV, Csermely P, **Schulc K***. MarkerPredict: predicting clinically relevant predictive biomarkers with machine learning. NPJ Systems Biology Applications 2025;11(1):132. , IF= 3.5, D1

   * *Corresponding author*

3. Kerestely M, Keresztes D, Szarka L, Kovacs BM, **Schulc K**, Veres DV, et al. System level network data and models attack cancer drug resistance. Br J Pharmacol. 2025:1–13., IF= 7.7, D1
4. Keresztes D, Kerestely M, Szarka L, Kovacs BM, **Schulc K**, Veres DV, et al. Cancer drug resistance as learning of signaling networks. Biomedical Pharmacotherapy. 2025; 183:117880. , IF= 7.5, D1
5. Veres T, Kerestely M, Kovacs BM, Keresztes D, **Schulc K**, Seitz E, et al. Cellular forgetting, desensitisation, stress and ageing in signalling networks. When do cells refuse to learn more? Cell Mol Life Sci. 2024;81(1):97. , IF= 6.2, D1
6. **Schulc K**. lncRNA signatures as biomarkers for the activity of oncogenic signaling pathways. Trilaterales Symposium; 09.24.; Heidelberg 2024.